HHS Public Access

Author manuscript

Biochem Biophys Res Commun. Author manuscript; available in PMC 2017 November 28.

Published in final edited form as:

Biochem Biophys Res Commun. 2011 October 07; 413(4): 555–560. doi:10.1016/j.bbrc.2011.08.137.

Endosomal trafficking of the G protein-coupled receptor somatostatin receptor 3

Cristy Tower-Gilchrist, **Eunjoo Lee**, and **Elizabeth Sztul***

Department of Cell Biology, University of Alabama at Birmingham, 1918 University Boulevard, McCallum 668, Birmingham, AL 35294, USA

Abstract

Intracellular trafficking of G protein-coupled receptors (GPCRs) regulates their surface availability and determines cellular response to agonists. Rab GTPases regulate membrane trafficking and identifying Rab networks controlling GPCR trafficking is essential for understanding GPCR signaling. We used real time imaging to show that somatostatin receptor 3 (SSTR3) traffics through Rab4-, Rab21-, and Rab11-containing endosomes, but largely bypasses Rab5 and Rab7 endosomes. We show that SSTR3 rapidly traffics through Rab4 endosomes but moves slower through Rab21 and Rab11 endosomes. SSTR3 passage through each endosomal compartment is regulated by the cognate Rab since expression of the inactive Rab4/S22N, Rab21/T33N, and Rab11/S25N inhibits SSTR3 trafficking. Thus, Rab4, Rab21, and Rab11 may represent therapeutic targets to modulate surface availability of SSTR3 for agonist binding. Our novel finding that Rab21 regulates SSTR3 trafficking suggests that Rab21 may play a role in trafficking of other GPCRs.

Keywords

Somatostatin receptor 3 (SSTR3); Rabs; Endosomes; Trafficking; Small GTPases

1. Introduction

GPCRs comprise the largest family of seven transmembrane-spanning surface receptors that mediate numerous physiological processes. Mutations in GPCR have been linked to human diseases, including Cushing's Syndrome, hormone dependent cancers, congestive heart failure, and diabetes [1]. Pathological mutations in GPCRs can cause the loss-of-function, gain of function, or relevant to this study, disrupt GPCR trafficking, thus perturbing downstream signaling pathways leading to disease [2].

GPCRs signaling is initiated when surface GPCRs bind agonist. After activation, GPCRs are endocytosed to terminate signal transduction, and subsequently are either recycled back to cell surface or targeted for degradation. In addition to agonist-induced trafficking, some

*Corresponding author. Fax: +1 205 975 9131. esztul@uab.edu (E. Sztul).

Appendix A. Supplementary data

Supplementary data associated with this article can be found, in the online version, at doi:10.1016/j.bbrc.2011.08.137.

GPCRs traffic in the absence of ligand and basal levels of receptor internalization have been observed that result in intracellular signaling [3]. Trafficking of GPCRs under basal conditions regulates the number of surface GPCRs and directly impacts the availability of agonist binding sites. Thus, it is essential to identify the molecular mechanisms that regulate basal trafficking of GPCRs.

Rab4, Rab5, Rab7, and Rab11 are known regulators of GPCRs traffic. Rab4 regulates trafficking of the neurokinin 1 receptor (NK1R), β2 adrenergic receptor (β2AR), and the oxytocin receptor [4–6]. Rab5 modulates trafficking of β2AR, NR1R, CXC chemokine receptor 2 (CXCR2), oxytocin receptor, and cannabinoid receptor 2 (CB2) [4–7]. Rab7 has been implicated in CXCR2 cycling [8]. Rab 11 regulates trafficking of M4 muscarinic acetylcholine receptor, vasopressin V2 receptor, and the CB2 receptor [7–9]. Recently, Rab22 has been shown to regulate endocytosis of the M4 muscarinic acetylcholine receptor [10]. Whether these Rabs regulate trafficking of other GPCRs and whether additional Rabs regulate GPCR trafficking remains under investigation.

Rab21 has been localized to early endosomes and the plasma membrane [11]. Rab21 appears to regulate endocytosis since cells expressing the inactive Rab21/T33N show decreased internalization and degradation of EGF and transferrin receptors [11]. Rab21 also regulates endocytosis of integrin-α5 and cell-extracellular matrix adhesion proteins [12]. Whether Rab21 participates in trafficking of GPCRs is unknown.

Five GPCRs, somatostatin receptors (SSTR1–5) bind somastotatin, a neuropeptide involved in neurotransmission and hormone secretion from the anterior pituitary gland, pancreas, and gastrointestinal tract [13]. The different SSTRs are found in different tissues and show distinct expression patterns during development [14]. SSTR3 has been localized to many regions of the rodent brain [15]. SSTR3 is concentrated in cilia in cultured hippocampal neurons and when expressed exogenously in polarized inner-medullary collecting duct (IMCD) cells [16,17]. SSTR3 is also detected on the plasma membrane of cells [18].

We used IMCD cells stably expressing SSTR3 and live imaging to probe SSTR3 distribution in endosomes, characterize the dynamics of SSTR3-containing endosomes, and assess the role of specific Rabs in SSTR3 trafficking through the endosomal network. We show that SSTR3 preferentially traffics through Rab4 and Rab21 early endosomes and through Rab11 recycling endosomes. We also show that SSTR3 moves more rapidly through Rab4 early endosomes than through Rab21 early endosomes and Rab11 recycling endosomes. SSTR3 trafficking requires functional Rabs because expression of dominant negative forms of Rab4, Rab21, and Rab11 inhibits SSTR3 trafficking. Our findings document the previously uncharacterized role of Rab4, Rab21, and Rab11 in endosomal trafficking of SSTR3. This extends the generality of Rab4 and Rab11 involvement in GPCR cycling. Our identification of Rab21 as a novel regulator of SSTR3 suggests that Rab21 might be a general facilitator of GPCR trafficking.

2. Materials and methods

2.1. Antibodies and reagents

Polyclonal anti-GFP antibody was from Abcam (catalog # ab290-50; Cambridge, MA). Monoclonal anti-acetylated tubulin was from Sigma (catalog # T6793; Saint Louis, Missouri). Alexa Fluor 594-goat anti-rabbit and Alexa Fluor 488-goat anti-mouse were from Invitrogen Molecular Probes, Inc. (Eugene, OR). Clones, primer sequences, and PCR conditions are available on request. Geneticin (G418) was from Gibco/Invitrogen Corporation (catalog number 11811-031; Carlsbad, CA).

2.2. DNA constructs

pEGFP-Rab21 wild-type and Rab21/T33N were from Dr. Jeremy Simpson (UCD Dublin Conway Institute of Biomolecular & Biomedical Research) [11] and subcloned into pmCherry-C1 (Clonetech) using BgIII and SacII. The primers to generate pmCherry-C1-tagged Rab21 wild-type and Rab21/T33N were 5′-GATCGAAGATCTATG CGACGACGA-3′ and 5′-GATCCCGCGGTTATCCAGAAGA-3′. DNA sequencing was performed by UAB Genomics Core Facility (Birmingham, AL). pmCherry-C2-Rab4a wild-type was from Dr. James Goldenring (Vanderbilt University Medical Center, Nashville, TN). It was mutagenized by PCR using primers 5′-GGAAATGCAGGA ACTGGCAAGAATTGCTTACTTCATCAGTTTATT-3′ and 5′-CAATAAA CTGATGAAGTAAGCAATTCTTGCCAGTTCCTGCATTTCC-3′ to generate pmCherry-C2-Rab4/S22N. All clones were verified by sequencing. DsRed-Rab11wild-type (#12679), DsRed-Rab11/S25N (#12680), mRFP-Rab5wild-type (#14437), and DsRed-Rab7 wild-type (#12661) were from Addgene and have been described [19,20].

2.3. Cell culture and transfections

Mouse IMCD3 cells were grown in Dulbecco's modified Eagles Medium/Ham's F12 50/50 (Mediatech, Comprehensive Cancer Center, UAB, Birmingham, AL) supplemented with 10% fetal bovine serum, 100 unit/mL penicillin/streptomycin, 1.2 g/L sodium bicarbonate, and 0.5 mM sodium pyruvate from Invitrogen Molecular Probes (Eugene, OR). IMCDs stably expressing EGFP-SSTR3 (SSTR3#1 IMCD3) were from Dr. Bradley Yoder (UAB, Birmingham, AL) and were cultured as above but supplemented with 200 μg/mL Geneticin. Cells were grown in 95% air and 5% CO_2 at 37 °C.

SSTR3#1 IMCD cells ($n = 5 \times 10^6$) were electroporated using BioRad Gene pulser II (Hercules, CA) with 10–20 μg DNA as in [17] and grown for 48–72 h before analysis.

2.4. Immunofluorescence microscopy and live cell imaging

Immunofluorescence was as in [21]. Dual color time-lapse imaging was performed on PerkinElmer Confocal System Ultra-VIEWERS 6FE-US equipped with 100× oil objective and processed/analyzed with Volocity 5.2. Images were acquired every 5 s over 10–20 min and movies were exported into Quicktime (Adobe Systems, Inc. San Jose, CA).

Pearson's correlation coefficients were calculated by Volocity software of z-stacked images. SSTR3 flux through endosomal compartments was assessed in 21–25 endosomes selected

from different cells by monitoring the Pearson's correlation coefficients within each endosome at 15 s intervals over 10 min.

3. Results

3.1. SSTR3 localization in IMCD cells

SSTR3 was detected in cilia where it co-localized with the ciliary marker acetylated tubulin (Fig. 1A, arrow), as described [17]. SSTR3 was also detected at the plasma membrane (Fig. 1A, arrowheads). In addition, confocal analysis shows SSTR3 in numerous punctate structures dispersed throughout the cell (Fig. 1B). The size and shape of these structures is consistent with endosomal compartments. Rabs show selectivity in their subcellular localization making them ideal compartment markers. Therefore we identified the SSTR3-containing compartments by determining their Rab content.

SSTR3 expressing IMCDs were transfected with distinct Rabs and co-localization between SSTR3 and each Rab was measured. SSTR3 co-localized extensively with the early endosomal Rab4, and almost every structure containing SSTR3 also contained Rab4 (Fig. 1C). Quantification of co-localization indicates a correspondingly high Pearson's coefficient (where a 0 value indicates no co-localization and a value of 1 indicates complete co-localization) of 0.861 (Fig. 1H). In contrast, SSTR3 showed only partial co-localization with Rab5 (Fig. 1D), with a relatively low Pearson's coefficient of 0.512 (Fig. 1H). SSTR3 also co-localized extensively with Rab21 (Fig. 1E), with a Pearson's coefficient of 0.823 (Fig. 1H). Thus, within early endosomal compartments SSTR3 appears to preferentially co-localize with Rab4 and Rab21, but largely segregates away from Rab5.

Early endosomes differentiate into late endosomes by loosing Rab5 and Rab4 and recruiting Rab7. SSTR3 shows almost no co-localization with Rab7 (Fig. 1F), with a Pearson's coefficient of 0.027 (Fig. 1H). Rab7 positive structures define a degradative pathway destined to lysosomes. The low levels of SSTR3 in Rab7 endosomes suggest that only a small proportion of SSTR3 is destined for degradation, in agreement with previous findings that only a small fraction of SSTR3 is targeted for degradation in neuroendocrine rat insulinoma and HEK 293 cells.

Strikingly, SSTR3 shows extensive co-localization with Rab11 (Fig. 1G), an established marker of recycling endosomes, with the highest Pearson's coefficient of 0.910 (Fig. 1H). Thus, SSTR3 localizes extensively to Rab4 and Rab21 early sorting endosomes and Rab11 recycling endosomes.

3.2. SSTR3 trafficking through Rab4, Rab21, and Rab11 endosomes

The localization of SSTR3 to early and recycling endosomes suggested that SSTR3 traffics through these compartments. We assessed the movement of SSTR3 through Rab4, Rab21, and Rab11 endosomes by real-time imaging in live cells.

SSTR3/Rab4-containing endosomes appear extremely dynamic and undergo continuous fusions and fissions (Fig. 2A and B; Movie 1). SSTR3 sorts within Rab4 endosomes as evidenced by the dynamic separation of small SSTR3-containing elements (green)

continuous with membranes containing Rab4 (yellow) (Fig. 2B, arrowheads). Often, numerous SSTR3-containing elements formed simultaneously from a single endosome (Fig. 2B). We also observed many elements containing exclusively SSTR3 and exclusively Rab4 (Fig. 2B, arrows).

To measure SSTR3 passage through Rab4 endosomes we performed a time-dependent co-localization coefficient analysis. We determined SSTR3 and Rab4 co-localization coefficients within 25 endosomes. The initial co-localization level was set at 1 and we counted endosomes as no longer having SSTR3 when their co-localization coefficient fell below 0.100. We reasoned that exit of SSTR3 (green) from Rab4 (red) endosomes will decrease the co-localization coefficient. Indeed, we observed SSTR3 segregating from Rab4, with more than half of the Rab4 endosomes loosing SSTR3 within 60 s (Fig. 2E). This suggests that SSTR3 rapidly moves through Rab4 endosomes.

SSTR3/Rab21 endosomes undergo short- and long-range movements between the cell center and periphery (Fig. 3A and B; Movie 2). SSTR3/Rab21 endosomes continuously fuse and fragment. Previous imaging of Rab21 in live cells treated with wortmanin showed Rab21 marking tubules emanating from Rab5 endosomes but did not characterize Rab21 behavior under normal conditions. Analysis of SSTR3 and Rab21 co-localization shows sub-domains containing only SSTR3 (green) or only Rab21 (red) in continuity with regions containing both proteins (yellow) (Fig. 3B, arrowheads). We also observed structures containing only SSTR3 adjacent to structures containing only Rab21 (Fig. 3B, arrows).

SSTR3 movement through the Rab21 endosome was measured by time-dependent co-localization coefficient within 21 endosomes. SSTR3 rapidly segregated from Rab21, with more than half of Rab21 endosomes loosing SSTR3 within 120 s (Fig. 3E). Thus, SSTR3 moves through Rab21 endosomes with a $t_{1/2}$ of 117 s, significantly slower than the $t_{1/2}$ of 51 s for SSTR3 passage through Rab4 endosomes (Supplemental Fig. S1A). To our knowledge this represents the first report of cargo traffic through Rab21 endosomes.

SSTR3/Rab11 endosomes also undergo rapid short- and long-range movements (Fig. 4A and B; Movie 3). Fusions and fragmentation of SSTR3/Rab11 endosomes were observed, consistent with reported Rab11 dynamics. SSTR3 and Rab11 show extensive subdomain segregation, with SSTR3 only (green) and Rab11-only (red) regions in continuity with SSTR3/Rab11 (yellow) elements (Fig. 4B, arrowheads). Often we observed elements containing only SSTR3 or only Rab11 (Fig. 4B, arrows).

SSTR3 passage through Rab11 endosomes was assessed by time-dependent co-localization analysis of 25 endosomes. SSTR3 clears from Rab11 endosomes with more than half of the Rab11 endosomes loosing SSTR3 within 180 s (Fig. 4E). This rate ($t_{1/2}$ ~ 159 s) is significantly slower than SSTR3 passage through Rab4 endosomes ($t_{1/2}$ ~ 51 s) and similar to SSTR3 passage through Rab21 endosomes ($t_{1/2}$ ~ 117 s) (Supplemental Fig. S1A).

3.3. SSTR3 traffic is regulated by Rab4, Rab21 and Rab11

All Rabs cycle between the active GTP-bound and the inactive GDP-bound form. Rab4/S22N assumes a conformation analogous to that of the inactive Rab4 and when transfected

into cells inhibits endosomal trafficking [22]. Expression of Rab4/S22N appears to decrease SSTR3 trafficking (Fig. 2C and D; Movie 4). We often observed SSTR3 (green) sub-domains that remain attached to Rab4/S22N-containing endosomes (Fig. 2D, arrowheads). Even after 150 s, a bud containing sorted SSTR3 did not disconnect from the globular endosome. Overall, SSTR3 remains within Rab4/S22N structures for prolonged times and SSTR3 is still detected in more than half of Rab4/S22N-positive endosomes after 360 s, giving a $t_{½}$ of ~461 s (Supplemental Fig. 1B). Thus, SSTR3 trafficking through early endosomes appears to require functional Rab4.

A dominant inactive Rab21/T33N causes defects in endocytosis of receptors and cell-extracellular matrix adhesion proteins [11,12]. Analysis of SSTR3 movement through Rab21/T33N endosomes shows that SSTR3 domains appear relatively stable (Fig. 3C and D, Movie 5). We often observed SSTR3 (green) separate into regions that remained attached to Rab21/T33N endosome (yellow) for long time (Fig. 3B, arrowheads). Occasionally, SSTR3 sorted from Rab21/T33N (Fig. 3B, arrows). Overall, SSTR3 movement through Rab21/T33N endosomes is decreased and SSTR3 is still detected in more than half of Rab21/T33N endosomes after 360 s, giving a $t_{½}$ of ~382 s (Supplemental Fig. 1B). Thus, SSTR3 trafficking through early endosomes appears to require functional Rab21.

The role of Rab11 in SSTR3 trafficking was explored by expressing the dominant negative Rab11/S25N that inhibits trafficking of transferrin and neonatal Fc receptor [23]. Expression of Rab11/S25N leads to slight fragmentation of structures containing SSTR3 and Rab11/S25N Fig. 4C). Analysis of SSTR3 movement through the Rab11/S25N endosome indicates that SSTR3 is delayed in exiting Rab11/S25N endosomes (Fig. 4C and D, Movie 6). While budding of SSTR3 (green) elements from Rab11/S25N endosomes (yellow) can be observed (Fig. 4D, arrowheads), the number of SSTR3 elements budding from Rab11/S25N endosomes is decreased. The majority of SSTR3 remains within Rab11/S25N endosomes for prolonged time. Rarely, we observed elements containing only SSTR3 or only Rab11/S25N (Fig. 4D, arrows). More than half of Rab11/S25N endosomes contain SSTR3 after 300 s, giving a $t_{½}$ of ~322 s (Supplemental Fig. 1B). Thus, efficient trafficking of SSTR3 requires functional Rab11.

4. Discussion

4.1. Endosomal trafficking of SSTR3

SSTR3 is a member of a family of five SSTRs encoded by distinct genes and differentially expressed in the brain and peripheral tissues [24]. The neuropeptide somatostatin binds to SSTR3 to regulate exocrine secretion and hormone release from a variety of endocrine cells, as well as modulate the responses of the central nervous system involved in locomotion and cognition. Somatostatin inhibits cell proliferation in multiple models of cancer, and analogs of somatostatin have been used as therapeutics in the treatment of neuroendocrine tumors [25]. Somatostatin action (and that of its clinically relevant analogs) relies on SSTR3 availability on cell surface, and this is governed by intracellular trafficking of SSTRs. Thus, characterizing the molecules that regulate SSTR trafficking might identify therapeutic targets for manipulating cellular responses to somatostatin (and its clinically relevant analogs).

SSTR3 expressed in RIN cells undergoes agonist-induced internalization in a process that involves AP2 and clathrin and is regulated by β-arrestin [26]. However, SSTR3 might also undergo basal cycling since SSTR3 can be detected within intracellular compartments even in the absence of agonist [26]. Basal cycling of SSTR3 regulates the level of surface SSTR3 and mediates the potential responsiveness of cells to agonist. Thus, it is essential to characterize the compartments through which SSTR3 moves and the molecular machinery that regulates SSTR3 movement under basal conditions.

Herein, we assessed endosomal trafficking of SSTR3 under basal conditions and identified Rab4, Rab21, and Rab11 as key regulators of SSTR3 movement. We show that SSTR3 co-localizes extensively with Rab4 and Rab21 and less with Rab5. Endosomal Rabs show spatial and temporal separation, and Rab4 and Rab5 show extensive co-localization but also areas of separation within a single endosomal compartment [27]. Rab21 co-localizes partially with Rab5 [11] and with Rab4 (data not shown), suggesting that it also defines a subdomain of the early endosome. The molecular mechanisms that govern the preferential localization of SSTR3 to the Rab4 and Rab21 subdomains remain to be investigated.

We show that SSTR3 also co-localizes with Rab11, in agreement with previous studies showing co-localization of internalized SSTR3 with Rab11 and with internalized transferrin, two markers of recycling endosomes [26]. In contrast, minimal amounts of SSTR3 co-localize with Rab7, a marker of late endosomes. Late endosomes receive cargoes targeted for degradation and the low levels of SSTR in this compartment suggest low degradative rate. This is consistent with previous reports that only ~20% of internalized SSTR3 is degraded while the vast majority recycles back to cell surface [26].

We assessed SSTR3 movement through endosomal compartments using real time dual color imaging. To our knowledge, this is first ever live analysis of SSTR3 movement within the endosomal pathway. We uncovered two pathways through the early endosome: a “fast” pathway out of the Rab4 compartment and a “slow” pathway from the Rab21 compartment. SSTR3 moves through the Rab4 compartment with a $t_{1/2}$ of ~51 s, significantly faster than through the Rab21 compartment with a $t_{1/2}$ of ~117 s. Interestingly, our data showing that SSTR3 can utilize “fast” and “slow” pathways at the early endosome, implies that the ratio of SSTR3 moving through the Rab4 or the Rab21 pathway may affect the number of surface exposed SSTR3. This in turn may affect the cells ability to bind and respond to somatostatin. Thus, the choice of the pathway taken by SSTR3 within early endosomes is likely to influence the signaling status of a cell.

SSTR3 co-localizes extensively with Rab11 suggesting that a significant proportion of cellular SSTR3 moves through recycling endosomes at steady state. SSTR3 movement through the Rab11 recycling endosome is relatively slow with a $t_{1/2}$ of 159 s. This is consistent with previous studies showing slower recycling from Rab11 endosomes than from early endosomes [28].

Previous studies have shown that Rab4, Rab5, Rab7, and Rab11 regulate internalization, degradation, and recycling of multiple GPCRs. Our study shows that the trafficking of a previously uncharacterized GPCRs, SSTR3 is also regulated by Rab4 and Rab11. Thus, our

findings further extend the generality of Rab4 and Rab11 function in GPCR trafficking. To our knowledge this represents the first analysis of the role these Rabs play in SSTR3 trafficking.

4.2. Rab21 role in GPCR trafficking

Rab21 localizes to early endosomes and functions therein to regulate trafficking of integrins and cell-extracellular matrix adhesion proteins and transferrin and EGF receptors [11,12]. The role for Rab21 in GPCR trafficking has not been previously explored. Here, we show that SSTR3 preferentially localizes to Rab21-containing subdomains of the early endosome and that active Rab21 is required for SSTR3 trafficking. Interestingly, SSTR3 movement through the Rab21 endosome is relatively slow, suggesting that unlike Rab4 which mediates “fast” recycling, Rab21 may facilitate a pathway that acts as a reservoir of SSTR3. This function might be analogous to the “slow” pathway regulated by Rab11 through the perinuclear recycling endosome. Rab21 has not been identified as a Rab affecting GPCR trafficking in previous studies and our report is the first to name Rab21 as a novel regulator of GPCR trafficking. Whether Rab21 regulates trafficking of only SSTR3, all SSTRs, a subset of GPCRs, or all GPCRs remains to be determined.

Our findings that Rab4, Rab21 and Rab11 play roles in SSTR3 trafficking have clinical relevance. SSTRs have been used to deliver radiolabeled or toxin-conjugated somatostatin analogs to tumor cells in a process that requires binding of the compounds to surface exposed SSTR and subsequent endocytosis [29]. The levels of SSTRs present on cell surface and available for ligand binding is the result of a delicate balance between SSTR endocytosis, recycling and degradation. Molecules that regulate these processes have the potential to influence SSTR exposure on cell surface and thus represent putative therapeutic targets. Currently, the identity of molecules that regulate SSTR trafficking is limited. Our findings on the requirement for Rab4, Rab21 and Rab11 in SSTR3 trafficking provides novel targets for manipulating SSTR3 flow within cells.

Supplementary Material

Refer to Web version on PubMed Central for supplementary material.

Acknowledgments

We thank Drs. Melanie Styers and Marlene Winklebauer for critical reading of this manuscript. We thank Dr. Bradley Yoder for providing IMCD cells stably expressing SSTR3 and reagents. This work was supported by P30 DK074038-03.

References

1. Jean-Alphonse F, Hanyaloglu AC. Regulation of GPCR signal networks via membrane trafficking. Mol. Cell Endocrinol. 2011; 331:205–214. [PubMed: 20654691]
2. Sorkin A, Von Zastrow M. Endocytosis and signalling: intertwining molecular networks. Nat. Rev. Mol. Cell Biol. 2009; 10:609–622. [PubMed: 19696798]
3. Chidiac P, Hebert TE, Valiquette M. Inverse agonist activity of beta-adrenergic antagonists. Mol. Pharmacol. 1994; 45:490–499. [PubMed: 7908406]

4. Roosterman D, Cottrell GS, Schmidlin F, et al. Recycling and resensitization of the neurokinin 1 receptor. Influence of agonist concentration and Rab GTPases. J. Biol. Chem. 2004; 279:30670–30679. [PubMed: 15128739]
5. Seachrist JL, Anborgh PH, Ferguson SS. Beta 2-adrenergic receptor internalization. Endosomal sorting, and plasma membrane recycling are regulated by rab GTPases. J. Biol. Chem. 2000; 275:27221–27228. [PubMed: 10854436]
6. Conti F, Sertic S, Reversi A, Chini B. Intracellular trafficking of the human oxytocin receptor: evidence of receptor recycling via a Rab4/Rab5. “Short cycle”. Am. J. Physiol. Endocrinol. Metab. 2009; 296:E532–E542. [PubMed: 19126785]
7. Grimsey NL, Goodfellow CE, Dragunow M. Cannabinoid receptor 2 undergoes Rab5-mediated internalization and recycles via a Rab11-dependent pathway. Biochim. Biophys. Acta. 2011; 1813:1554–1560. [PubMed: 21640764]
8. Fan GH, Lapierre LA, Goldenring JR, Richmond A. Differential regulation of CXCR2 trafficking by Rab GTPases. Blood. 2003; 101:2115–2124. [PubMed: 12411301]
9. Innamorati G, Le Gouill C, Balamotis M, Birnbaumer M. The long and the short cycle. Alternative intracellular routes for trafficking of G-protein-coupled receptors. J. Biol. Chem. 2001; 276:13096–13103. [PubMed: 11150299]
10. Reiner C, Nathanson NM. The internalization of the M2 and M4 muscarinic acetylcholine receptors involves distinct subsets of small G-proteins. Life Sci. 2008; 82:718–727. [PubMed: 18295803]
11. Simpson JC, Griffiths G, Wessling-Resnick M, et al. A role for the small GTPase Rab21 in the early endocytic pathway. J. Cell Sci. 2004; 117:6297–6311. [PubMed: 15561770]
12. Pellinen T, Arjonen A, Vuoriluoto K, et al. Small GTPase Rab21 regulates cell adhesion and controls endosomal traffic of beta1-integrins. J. Cell Biol. 2006; 173:767–780. [PubMed: 16754960]
13. Jacobs S, Schulz S. Intracellular trafficking of somatostatin receptors. Mol. Cell Endocrinol. 2008; 286:58–62. [PubMed: 18045773]
14. Barnett P. Somatostatin and somatostatin receptor physiology. Endocrine. 2003; 20:255–264. [PubMed: 12721505]
15. Handel M, Schulz S, Stanarius A, et al. Selective targeting of somatostatin receptor 3 to neuronal cilia. Neuroscience. 1999; 89:909–926. [PubMed: 10199624]
16. Berbari NF, Bishop GA, Askwith CC, et al. Hippocampal neurons possess primary cilia in culture. J. Neurosci. Res. 2007; 85:1095–1100. [PubMed: 17304575]
17. Berbari NF, Johnson AD, Lewis JS, et al. Identification of ciliary localization sequences within the third intracellular loop of G protein-coupled receptors. Mol. Biol. Cell. 2008; 19:1540–1547. [PubMed: 18256283]
18. Roosterman D, Roth A, Kreienkamp HJ, et al. Distinct agonist-mediated endocytosis of cloned rat somatostatin receptor subtypes expressed in insulinoma cells. J. Neuroendocrinol. 1997; 9:741–751. [PubMed: 9355043]
19. Choudhury A, Dominguez M, Puri V, et al. Rab proteins mediate Golgi transport of caveola-internalized glycosphingolipids and correct lipid trafficking in Niemann-Pick C cells. J. Clin. Invest. 2002; 109:1541–1550. [PubMed: 12070301]
20. Vonderheit A, Helenius A. Rab7 associates with early endosomes to mediate sorting and transport of Semliki forest virus to late endosomes. PLoS Biol. 2005; 3:e233. [PubMed: 15954801]
21. Tower C, Fu L, Gill R, et al. Human cytomegalovirus UL97 kinase prevents the deposition of mutant protein aggregates in cellular models of Huntington’s disease and ataxia. Neurobiol. Dis. 2011; 41:11–22. [PubMed: 20732421]
22. van der Sluijs P, Hull M, Webster P, et al. The small GTP-binding protein rab4 controls an early sorting event on the endocytic pathway. Cell. 1992; 70:729–740. [PubMed: 1516131]
23. Ward ES, Martinez C, Vaccaro C, et al. From sorting endosomes to exocytosis: association of Rab4 and Rab11 GTPases with the Fc receptor. FcRn, during recycling. Mol. Biol. Cell. 2005; 16:2028–2038. [PubMed: 15689494]
24. Reisine T, Bell GI. Molecular biology of somatostatin receptors. Endocr. Rev. 1995; 16:427–442. [PubMed: 8521788]

25. Reubi JC, Waser B, Cescato R, et al. Internalized somatostatin receptor subtype 2 in neuroendocrine tumors of octreotide-treated patients. J. Clin. Endocrinol. Metab. 2010; 95:2343–2350. [PubMed: 20228164]

26. Kreuzer OJ, Krisch B, Déry O, et al. Agonist-mediated endocytosis of rat somatostatin receptor subtype 3 involves beta-arrestin and clathrin coated vesicles. J. Neuroendocrinol. 2001; 13:279–287. [PubMed: 11207943]

27. Sönnichsen B, De Renzis S, Nielsen E, et al. Distinct membrane domains on endosomes in the recycling pathway visualized by multicolor imaging of Rab4, Rab5, and Rab11. J. Cell Biol. 2000; 149:901–914. [PubMed: 10811830]

28. Stenmark H. Rab GTPases as coordinators of vesicle traffic. Nat. Rev. Mol. Cell Biol. 2009; 10:513–525. [PubMed: 19603039]

29. Colao A, Faggiano A, Pivonello R. Somatostatin analogues: treatment of pituitary and neuroendocrine tumors. Prog. Brain Res. 2010; 182:281–294. [PubMed: 20541670]

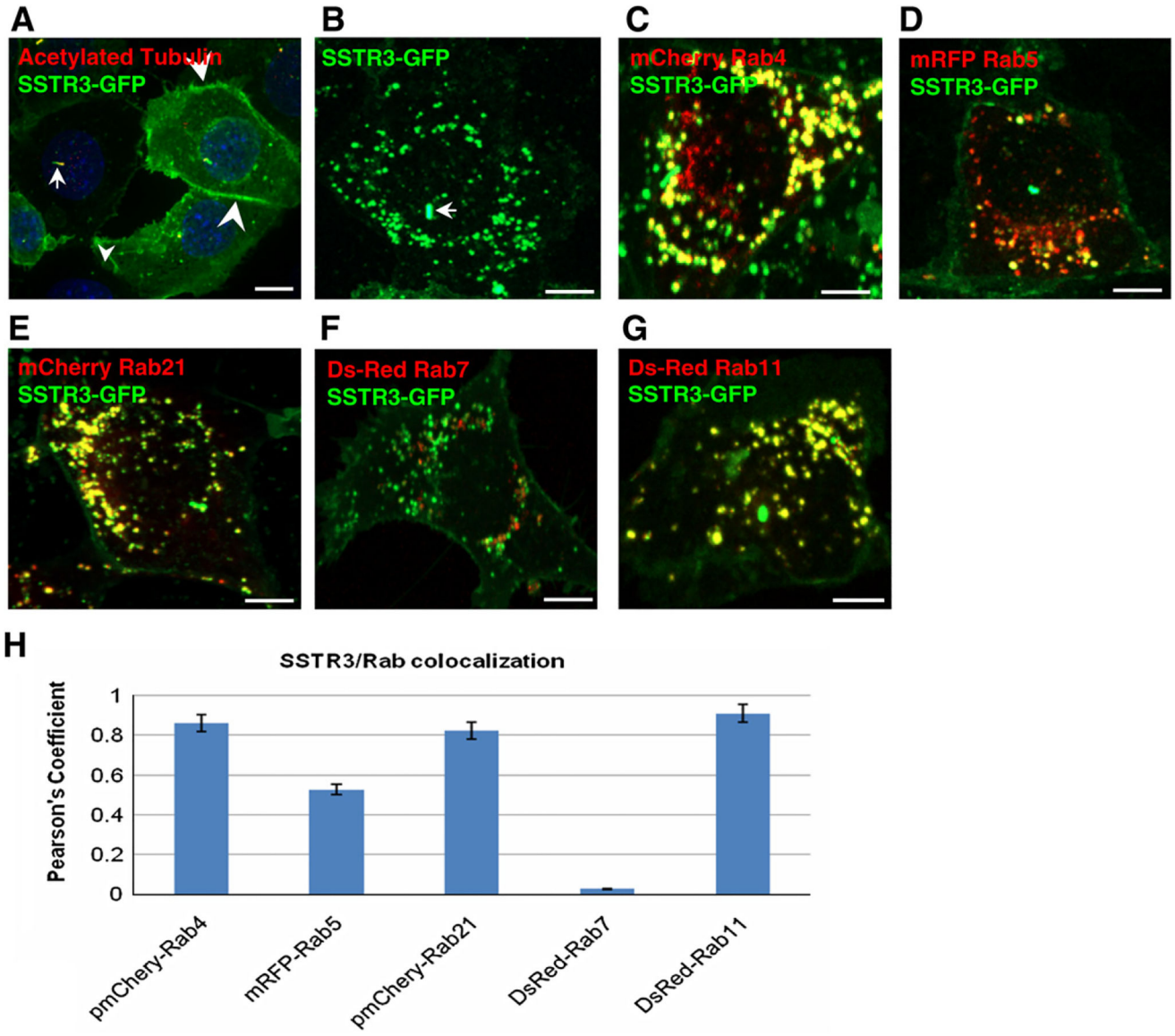

Fig. 1.

SSTR3 localizes to endosomes in IMCD cells. (A and B) IMCD cells expressing EGFP-SSTR3 were processed for IF with anti-GFP antibodies (to detect SSTR3) and acetylated tubulin (to detect cilia) (A) or imaged directly (B). (C–G) EGFP-SSTR3 expressing cells were transfected with mCherry Rab4 (C), mRFP-Rab5 (D), mCherry Rab21 (E), Ds-red Rab7 (F), or Ds-Red Rab11 (G) and imaged after 48 h. (H) The level of co-localization of SSTR3 with each Rab was determined by Pearson's Correlation Coefficient. SSTR3 localizes to cilia (arrow in A and B), plasma membrane (arrowheads in A) and early and recycling endosomes (C and E). Bars, 10 μm (A) and 19 μm (B–G). (For interpretation of the references to color in this figure legend, the reader is referred to the web version of this article.)

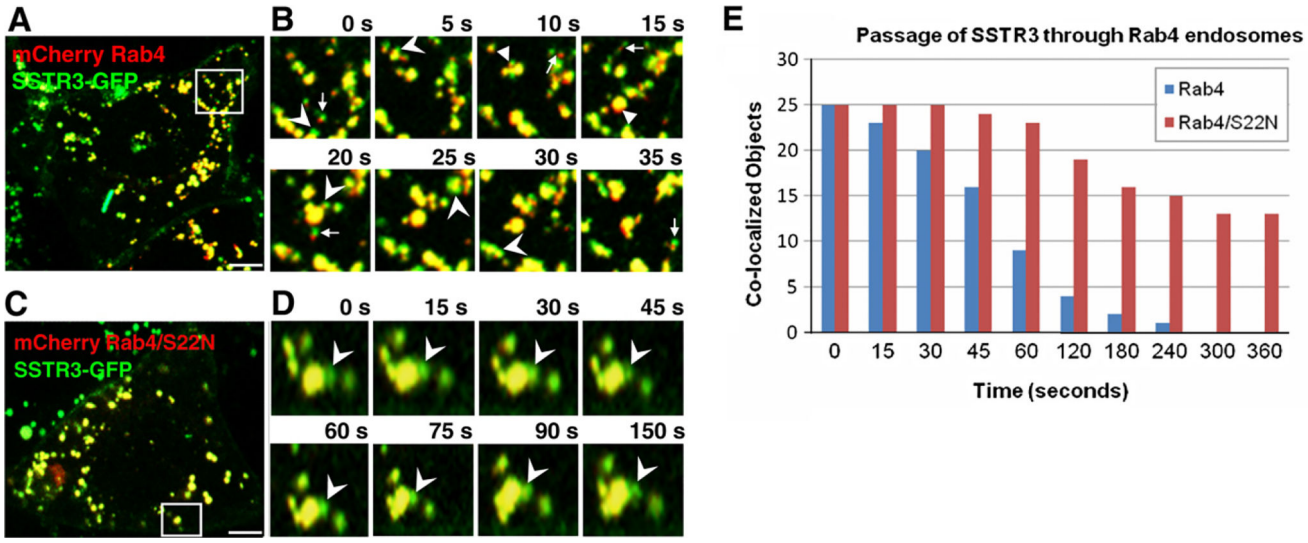

Fig. 2.

SSTR3 trafficking is regulated by Rab4. EGFP-SSTR3 expressing IMCD cells were transfected with mCherry Rab4 (A and B) or mCherry Rab4/S22N (C and D). After 48 h cells were imaged and consecutive images of cell regions outlined in A and C are presented in B and D, respectively. Arrowheads point to SSTR3 (green) separating from Rab4-containing (yellow) endosomes. Arrows point to SSTR3 only (green) elements separated from Rab4 only (red) elements. (E) SSTR3 separation from Rab4 or Rab4/S22N was measured by determining the co-localization coefficient between SSTR3 and Rab4 or Rab4/S22N as a function of time in 25 SSTR3/Rab4 or SSTR3/Rab4/S22N endosomes. Bars, 19 μm. (For interpretation of the references to color in this figure legend, the reader is referred to the web version of this article.)

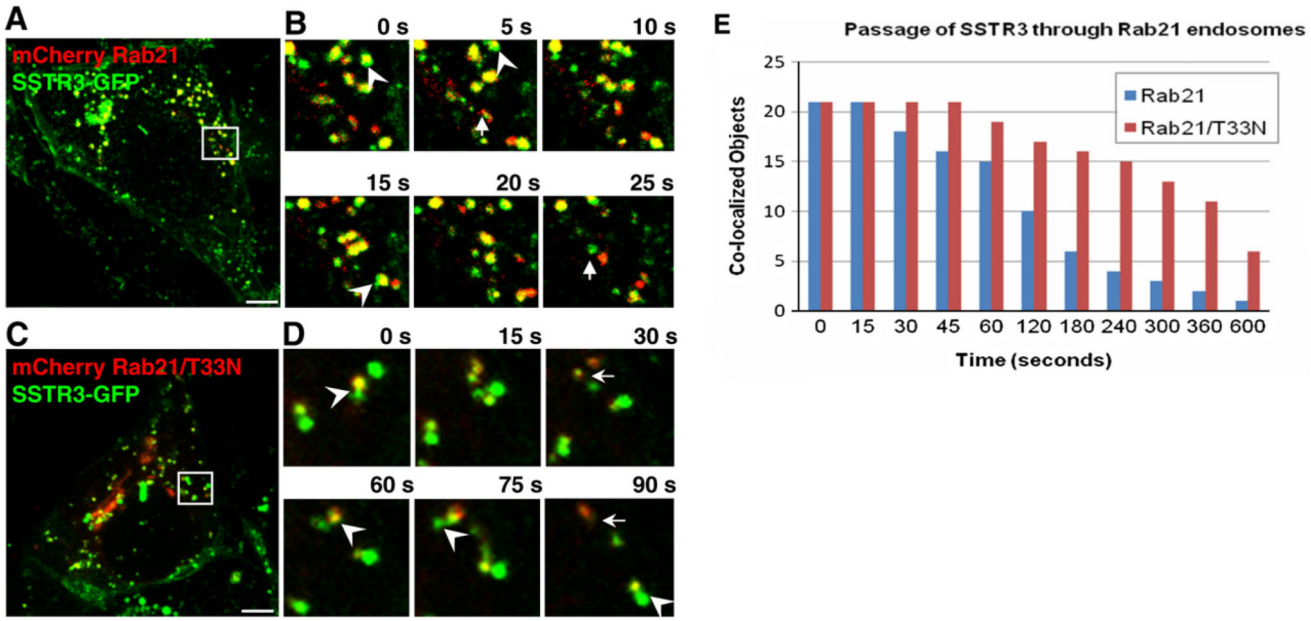

Fig. 3.

SSTR3 trafficking is regulated by Rab21. EGFP-SSTR3 expressing IMCD cells were transfected with mCherry-Rab21 (A and B) or mCherry-Rab21/T33N (C and D). After 48 h cells were imaged and consecutive images of cell regions outlined in A and C are presented in B and D, respectively. Arrowheads point to SSTR3 (green) separating from Rab21-containing (yellow) endosomes. Arrows point to SSTR3 only (green) elements separated from Rab21 only (red) elements. (E) SSTR3 separation from Rab21 or Rab21/T33N was measured by determining the co-localization coefficient between SSTR3 and Rab21 or Rab21/T33N as a function of time in 21 SSTR3/Rab21 or SSTR3/Rab21/T33N endosomes. Bars, 19 μm. (For interpretation of the references to color in this figure legend, the reader is referred to the web version of this article.)

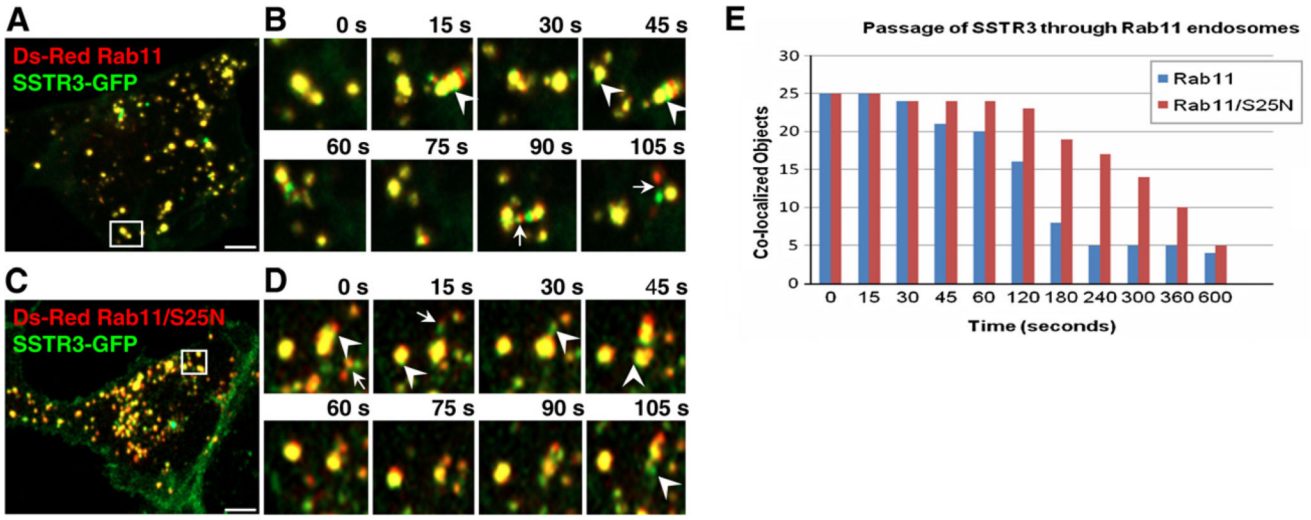

Fig. 4.

SSTR3 trafficking is regulated by Rab11. EGFP-SSTR3 expressing IMCD cells were transfected with DsRed Rab11 (A and B) or DsRed Rab11/S25N (C and D). After 48 h cells were imaged and consecutive images of cell regions outlined in A and C are depicted in B and D, respectively. Arrowheads point to SSTR3 (green) separating from Rab11-containing (yellow) endosomes. Arrows point to SSTR3 only (green) elements separated from Rab11 only (red) elements. (E) SSTR3 separation from Rab11 and Rab11/S25N was measured by determining the co-localization coefficient between SSTR3 and Rab11 or Rab11/S25N as a function of time in 25 SSTR3/Rab11 or SSTR3/Rab11/S25N endosomes. Bars, 19 μm. (For interpretation of the references to color in this figure legend, the reader is referred to the web version of this article.)